

# Organoclay-modified thermotropic liquid crystalline polymers as viscosity reduction agents for high molecular mass polyethylene

Youhong Tang · Ping Gao · Lin Ye ·  
Chengbi Zhao

Received: 3 March 2010 / Accepted: 29 April 2010 / Published online: 14 May 2010  
© Springer Science+Business Media, LLC 2010

**Abstract** Small amounts of organoclays of different sizes and concentrations were added into thermotropic liquid crystalline polymer (TLCP) forming four types of organoclay-modified TLCPs (TC3 white, TC3 dark, TC3 FS, and TC3 UP), which had different rheological behaviors in the nematic temperature region of TLCP. Acting as viscosity reduction agents, 1.0 wt% of each organoclay-modified TLCPs were blended with high molecular mass polyethylene (HMMPE), respectively. The organoclay-modified TLCP/HMMPE blends displayed different rheological properties from each other or compared with HMMPE and 1.0 wt% TLCP/HMMPE blend [PT1]. The organoclay-modified TLCPs had greater viscosity reduction efficiency than the original TLCP in HMMPE, a lower yielding stress and yielding start shear rate, and a narrower yielding transition region than those of PT1. The

rheological performance of the blends, 1.0 wt% TC3 white/HMMPE, 1.0 wt% TC3 FS/HMMPE, and PT1, could be successfully described by a binary flow pattern model.

## Introduction

Adding thermotropic liquid crystalline polymers (TLCPs) into engineering polymers matrix is known to reduce polymer matrix viscosity [1–3] as well as to improve its mechanical and barrier properties [4]. TLCP, acting as a viscosity reduction agent, should be used in the nematic phase, though some cases, TLCP in the smectic phase also has viscosity reduction effects in polymer melts [2]. The effect of a small TLCP loading dramatically changing the bulk viscosity of thermoplastics with high efficiency has seldom been reported [5–9]. Viscosity reductions of ~93% and ~89% were observed at 185 °C when the TLCP was a fully nematic phase and at 220 °C when the TLCP was a nematic–isotropic biphasic, when 2.0 wt% TLCP was added into high density polyethylene (HDPE). HDPE extrudate distortion and melt fracture were completely eliminated for apparent shear rates up to 1000 s<sup>-1</sup> at 185 °C [5, 7]. It was also shown that a small amount of TLCP (1.0 wt%) added to high molecular weight polyethylene (HMMPE, TR570) produced a dramatic reduction in bulk viscosity (>95.0%) at 190 °C, when the TLCP was in its nematic phase structure. A significant improvement in extrudate surface smoothness has also been observed, coupled with an increase in processing window from 34 s<sup>-1</sup> to up to 1000 s<sup>-1</sup> [6, 9]. A dramatic reduction in bulk viscosity (>98.4%) was also achieved when 3.0 wt% TLCP and 1.0 wt% organoclay was blended in HMMPE under an appropriate fabrication sequence of adding two

---

Y. Tang · P. Gao (✉)  
Department of Chemical and Biomolecular Engineering,  
The Hong Kong University of Science and Technology,  
Clear Water Bay, Kowloon, Hong Kong, China  
e-mail: kepgao@ust.hk

L. Ye  
Centre for Advanced Materials Technology,  
School of Aerospace, Mechanical and Mechatronic Engineering,  
The University of Sydney, Sydney, NSW 2006, Australia

Y. Tang (✉) · C. Zhao  
Centre for Advanced Marine Materials, School of Civil  
Engineering and Transportation, South China University  
of Technology, Guangzhou 510641, China  
e-mail: youhongtang@gmail.com

fillers (organoclay and TLCP). Moreover, the processing window was increased from  $39.6 \text{ s}^{-1}$  to more than  $500.0 \text{ s}^{-1}$  in terms of shear rate [10, 11].

Four typical TLCP/organoclay hybrid systems have been reported previously [12]. Organoclays of different concentrations and sizes formed different morphologies in the TLCP matrix, generating different rheological properties. The TLCP modified with 3.0 wt% as-received organoclay [TC3 UP] system [12] was separated by a capillary rheometer at a low shear rate into two parts; one was TC3 white, which was the extruded part, the other was TC3 dark, which was left in the barrel. The TC3 white was a fully exfoliated organoclay-modified TLCP with uniform organoclay size of 15–25 nm, which did not affect the liquid crystallinity and mesophase of the TLCP in the nematic state, but it enhanced the rigidity of the TLCP. TC3 white had even lower viscosity and the first normal stress different (N1) values but larger N1 slopes than those of the pure TLCP [12]. TC3 dark has a typical model structure of TLCP molecules intercalated into layered silicate galleries. In one part, the TLCP molecules were confined in organoclay galleries, where the thermal stability of the TLCP was dramatically enhanced. In the other part, the organoclay formed small clusters and disrupted the TLCP mesophase structures, and then the thermal stability of the TLCP was decreased. TC3 dark had more than three orders of magnitude higher apparent shear viscosity than that of the TLCP in the linear viscoelastic region, but after steady shear, the shear viscosity decreased to less than two orders of magnitude higher than that of TLCP [12]. After wet ball milling and ultrasonication treated the as-received organoclay, 3.0 wt% the treated-organoclay in TLCP formed TC3 FS. In this modified TLCP system, organoclays were 100–200 nm in size, which was comparable with the fully extended size of the TLCP molecule, i.e., 85 nm. The treated-organoclay formed partially intercalated morphologies in the TLCP with a cluster size of 10–20 nm. TC3 FS displayed just below one order of magnitude greater apparent shear viscosity than that of TLCP and had a less negative effect on the liquid crystallinity of the TLCP [12].

On the basis of the studies described above, it is considered that TLCPs, appropriately modified by organoclays, may be promising viscosity reduction agents for polyethylene (PE). In this study, four typical TLCP/organoclay hybrids (TC3 white, TC3 dark, TC3 UP, and TC3 FS) are used with a concentration of 1.0 wt% in the PE matrix and performance of the organoclay-modified TLCP/PE blends are characterized by rheological and morphological methods. For comparisons, purified TLCP of 1.0 wt% in PE [PT1] is also prepared and characterized. Finally, a binary model is used to describe the rheological behaviors of some of these blends, with excellent consistency of results.

## Experimental

### Materials and sample preparation

The HMMPE, Marlex HXM TR571, used in this study was kindly supplied by Philips Petroleum International Inc., USA. The melt index of TR571 is 2.5 g/10 min (ASTM D1238, 190 °C/2.16 kg). TLCP is a main chain copolyester containing of mole fractions of 30% *p*-hydroxybenzoic acid, 35% hydroquinone, and 35% sebacic acid (HAB/HQ/SA). It was synthesized and kindly supplied by B. P. Chemicals Ltd., UK. The organoclay, Cloisite 20A, is a natural montmorillonite modified with dimethyl dihydrogenated tallow alkyl quaternary ammonium chloride, supplied by Southern Clay Products, USA. Detailed information about the preparation of the four organoclay-modified TLCPs (TC3 white, TC3 dark, TC3 UP, and TC3 FS) and purification of the as-received TLCP used in this study has been elaborated in the previous study [12]. That is, 3 wt% as-received organoclay/as-received TLCP [TC3 UP], 3 wt% treated organoclay/as-received TLCP [TC3 FS] have been prepared by a combination of ultrasonication, centrifugation, and solution casting methods. TC3 white and TC3 dark have been prepared by using shear-induced phase phenomenon of TC3 UP. TC3 UP was extruded using a capillary rheometer (Göttfert Rheograph 2003A, Germany) at 190 °C at a low speed (5.0 l/s).

For the blends, the dried organoclay-modified TLCPs (or purified TLCP) in powder form and the HMMPE in pellet form were mechanically pre-mixed at room temperature until macroscopically homogeneous. The mixture was then extruded using a Dr. Collin twin screw extruder (Dr. Collin GMBH, Germany) at 190 °C with three extrusions at different speeds (75, 300, and 300 rad/s, respectively). The extrudate was palletized and kept dry inside an oven overnight to remove moisture formed during processing. Five blends were prepared: 1.0 wt% TLCP/HMMPE [PT1], 1.0 wt% TC3 white/HMMPE [P(TC3 white 1%)], 1.0 wt% TC3 dark/HMMPE [P(TC3 dark 1%)], 1.0 wt% TC3 FS/HMMPE [P(TC3 FS 1%)], and 1.0 wt% TC3 UP/HMMPE [P(TC3 UP 1%)].

### Characterization methods

Wide angle X-ray diffraction (WAXRD) was conducted at room temperature using a Philips powder X-ray diffraction system (Model PW 1830, The Netherlands). WAXRD was conducted with Cu K $\alpha$  radiation of wavelength 1.5406 Å. The organoclay-modified TLCPs embedded in epoxy were ultra-microtomed on an ultracut microtome (Leica ultracut-R ultramicrotome, Germany) at room temperature to produce sections with nominal thickness of 100 nm. Transmission electron microscopy (TEM) images were obtained

at 200 kV with a transmission electron microscope (JEOL 2010, Japan).

Controlled strain rheological measurements were carried out using an Advanced Rheometric Expansion System (ARES) (TA Instruments, USA) with a 200 g cm transducer within the resolution limit of 0.02 g cm. Fifty millimeters of parallel plate fixtures were used for all the characterizations of TLCP and organoclay-modified TLCPs reported here. Twenty-five millimeters of parallel plate fixtures were used for all the characterizations of HMMPE and its blends. All measurements were performed at 185 °C in N<sub>2</sub> atmosphere for the TLCP and organoclay-modified TLCPs, where the TLCP exhibited stable rheological properties in the nematic phase. The HMMPE and its blends were tested at 190 °C. Before testing, the equipment was preheated and equilibrated at the test temperature for at least 30 min.

The rheological behaviors of HMMPE and its blends were also characterized by a capillary rheometer (Göttfert Rheograph 2003A, Germany) at 190 °C. Here, the controlled piston speed mode was used with round hole capillary dies (nominal  $L/D$  ratio equals to 30/1 and die entrance angle of 180°). The die diameters used here were recalibrated before use by using optical microscopy with controllable position to measure the diameter of dies and confirmed by using PS and PMMA as basic materials for Rabinowitsch and Bagley correction (calibrated die diameters of  $D = 0.924$  and  $0.542$  mm for nominal  $D = 1.0$  and  $0.7$  mm dies). All the samples were dried in an oven at 105 °C for at least 12 h before testing. The presented data have already been corrected by Rabinowitsch and Bagley correction.

The morphology of the extrudates generated during the capillary rheometer experiment was examined by high resolution scanning electron microscope (SEM) (JEOL 6700F, Japan) with the acceleration voltage 5 kV. All samples were sputter-coated with a  $\sim 200$  Å layer of gold to minimize charging. The samples were quenched by compressed air from a hose placed near the die exit, providing a cooling ring. This ‘froze’ the structure of the TLCP droplets or fibrils before they could relax completely. Micrographs of the surfaces of these samples were taken after etching with a 10 wt% aqueous sodium hydroxide solution at 75 °C for 30 min.

## Result and discussion

### Dispersion of organoclays

The dispersion of organoclays in organoclay-modified TLCPs has already been characterized by WAXRD and TEM in our earlier study [12]. In TC3 white, the (001)

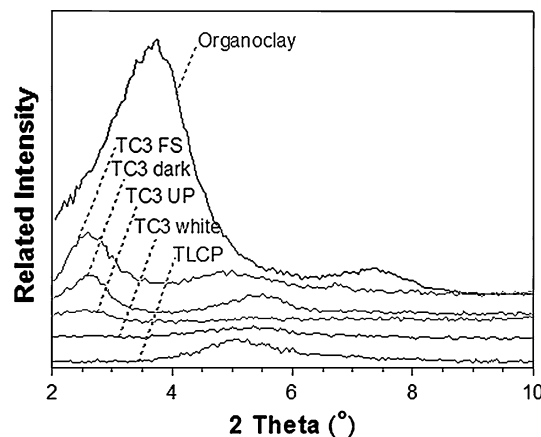


**Fig. 1** WAXRD patterns of organoclay, TLCP, and organoclay-modified TLCP blends

plane diffraction peak observed in the XRD pattern disappeared, compared with the pattern of as-received organoclay with  $d$ -spacing of 2.35 nm, as shown in Fig. 1. This observation suggests that the organoclay layer distance in TC3 white may become larger than that of as-received organoclay, due to either the formation of an exfoliated structure in the TLCP matrix, or to the heavy agglomeration of organoclay, or simply to the low concentration of organoclay. The corresponding peaks in TC3 dark and TC3 FS shifted to higher values of 3.27 and 3.40 nm, respectively, as the gallery expanded to accommodate the intercalating polymer. The corresponding XRD peak of TC3 UP also displayed a lower angle but took the form of a plateau with low intensity rather than a sharp peak. This suggested that the spaces between layers in the TC3 UP became larger than the as-received organoclay and formed a partially intercalated structure in the TLCP.

XRD and TEM are complementary techniques, in that one technique can provide information missed by the other in analyzing the morphology of layered silicates in polymeric matrix, especially for exfoliated structures. Typical TEM photographs of organoclay-modified TLCP blends were reported before [12] and also shown in Figs. 2–5. In Fig. 2 for TC3 white, the dark plates, 15–25 nm in length, are the organoclays with surfaces paralleling the observed plane. The organoclays were fully exfoliated and well dispersed in the TLCP matrix without any agglomeration. Bright field TEM images of TC3 dark and TC3 FS are shown in Figs. 3 and 4. Small magnification graphs (Figs. 3a, 4a) show the dispersion of the organoclays in the polymer matrix at both magnification levels, with most displaying agglomerations of size 20–50 nm for TC3 dark and 10–20 nm for TC3 FS. The peaks in the XRD patterns are attributed to the agglomerated layers. The periodic alternating dark and light bands represent the layers of organoclay and the interlayers, respectively, with about

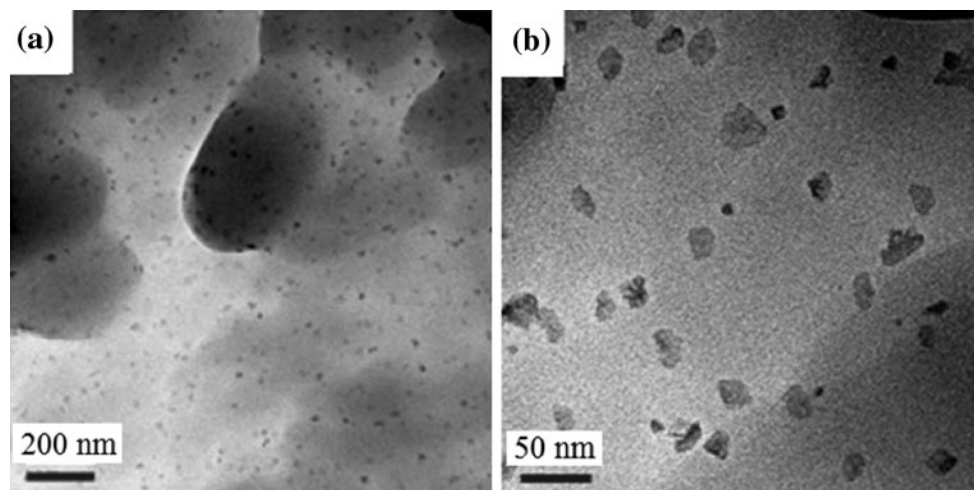


**Fig. 2** TEM images of TC3 white with different magnifications

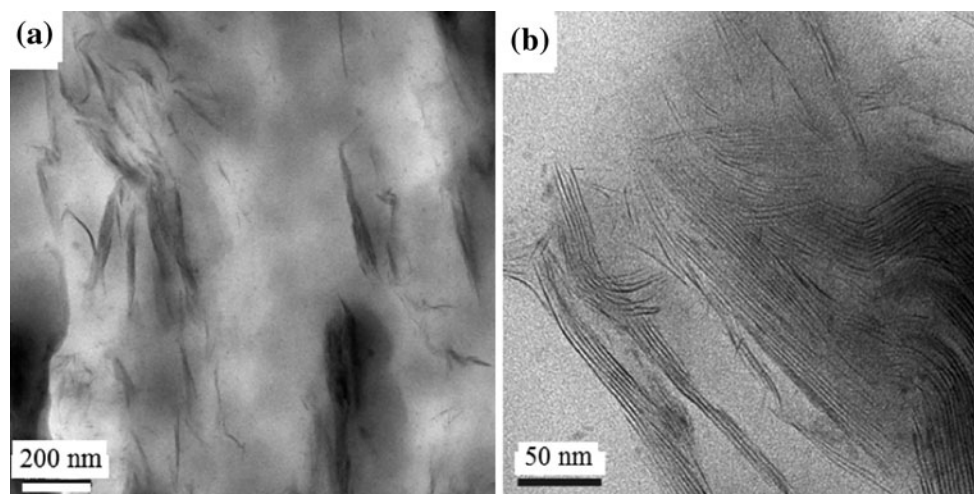


**Fig. 3** TEM images of TC3 dark with different magnifications

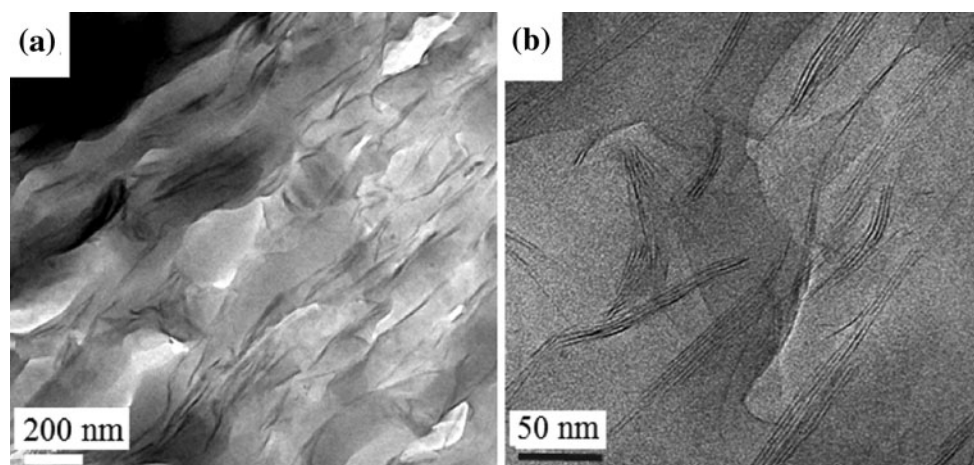


**Fig. 4** TEM images of TC3 FS with different magnifications

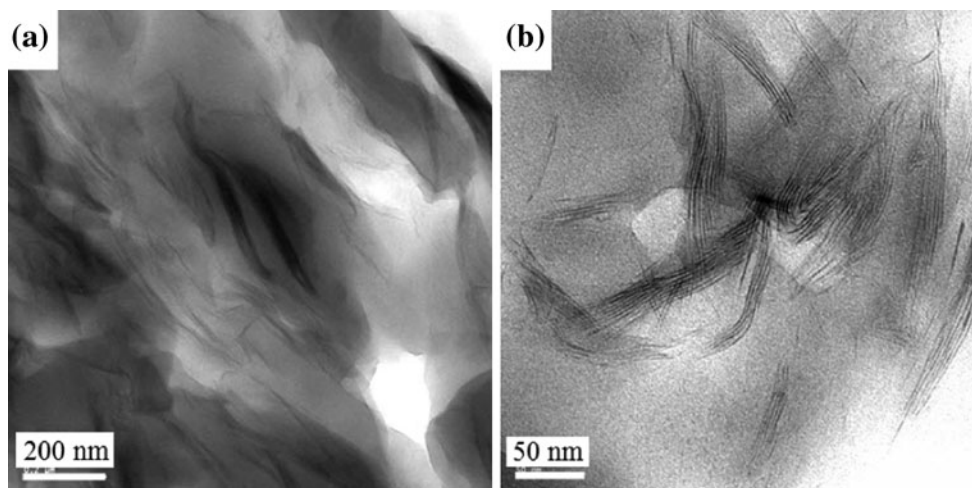


**Fig. 5** TEM images of TC3 UP with different magnifications

3 nm between the organoclay layers (Figs. 3b, 4b). The as-received organoclay exhibited the same microstructure as that observed in Figs. 3b and 4b but with a smaller inter-layer spacing. Moreover, Fig. 4b shows that the organoclay size is uniform and within the range of 100–200 nm, which is comparable with the chain length of a fully extended TLCP molecule based on its number average molecular mass of 14,000 kg/kmol, i.e.,  $\sim 85$  nm [9]. For the TC3 UP, organoclays were well dispersed in the TLCP with some agglomeration of about 50 nm in size, as shown in Fig. 5a. Figure 5b displays high magnification images of TC3 UP which show that the clay formed partially intercalated structures with  $d$ -spacing approximately 4–5 nm on average; the presence of the broad shoulder in the XRD pattern is attributed to these non-exfoliated layers which are parallel in the agglomerated layers.

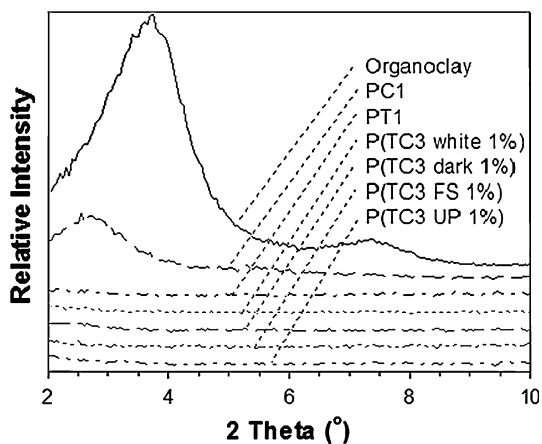


**Fig. 6** WAXRD patterns of organoclay and HMMPE blends: 1.0 wt% organoclay/HMMPE [PT1], 1.0 wt% TLCP/HMMPE [PC1], 1.0 wt% TC3 white/HMMPE [P(TC3 white 1%)], 1.0 wt% TC3 dark/HMMPE [P(TC3 dark 1%)], 1.0 wt% TC3 FS/HMMPE [P(TC3 FS 1%)], 1.0 wt% TC3 UP/HMMPE [P(TC3 UP 1%)]

Here, dispersions of organoclay-modified TLCPs in the PE matrix were characterized by WAXRD. In Fig. 6, as-received organoclay and 1.0 wt% organoclay/PE blend [PC1] demonstrate peaks in the WAXRD pattern, with  $d$ -spacing corresponding to 2.35 and 3.46 nm, respectively. Other blends do not show any peaks in the measured regions. This phenomenon was not caused by fully exfoliated structures of organoclay in the blends, but was due to small concentrations of organoclay in the matrix. It is clearly shown that no dramatic surface agglomeration occurred in the blends during the processing.

#### Linear viscoelasticity behaviors

Complex viscosities of organoclay-modified TLCPs and HMMPE blends from dynamic frequency sweep tests are exhibited in Figs. 7 and 8 separately. In Fig. 7, with differently modified organoclays (different sizes and concentrations), TLCP exhibits totally different viscoelastic behavior in the linear viscoelastic region. Compared to the apparent shear viscosity of the purified TLCP, at the frequency of 10.0 rad/s, the apparent shear viscosity of TC3 dark is almost four orders of magnitude higher, that of TC3 UP is more than two orders of magnitude higher, and that of TC3 FS is more than one order of magnitude higher. However, the apparent shear viscosity of TC3 white is similar to that of purified TLCP. Meanwhile, TC3 dark and TC3 UP have similar rheological curves and TC3 white and purified TLCP have similar rheological curves. TC3 FS shows a similar rheological curve to that of TC3 dark and TC3 UP in the low frequency region and a similar rheological curve to that of TC3 white and purified TLCP in the high frequency region.

In Fig. 8, little difference is evident in the curves of the HMMPE blends, which means that the small amounts of TLCP and organoclay-modified TLCPs in those blends

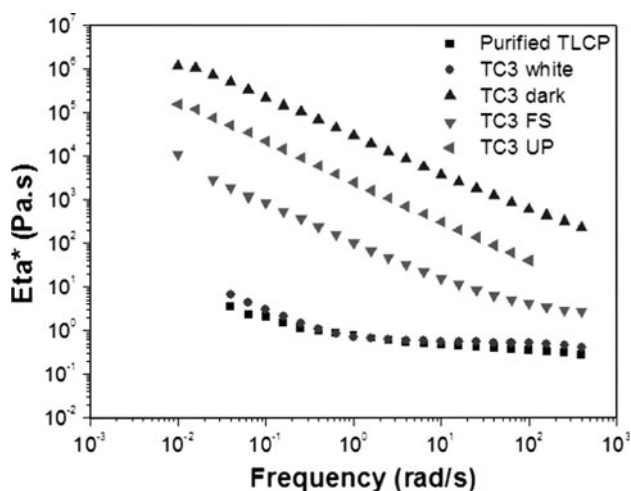


**Fig. 7** Dynamic frequency sweep at 185 °C for purified TLCP and organoclay-modified TLCPs: TC3 white, TC3 dark, TC3 FS, and TC3 UP

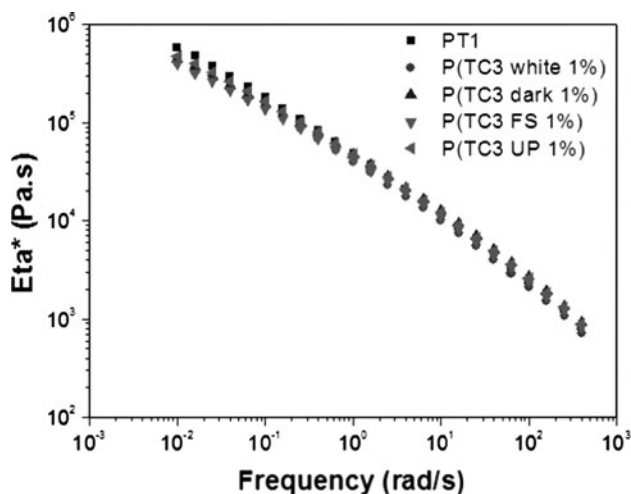


**Fig. 8** Dynamic frequency sweep at 190 °C for HMMPE blends: 1.0 wt% TLCP/HMMPE [PT1], 1.0 wt% TC3 white/HMMPE [P(TC3 white 1%)], 1.0 wt% TC3 UP/HMMPE [P(TC3 UP 1%)], 1.0 wt% TC3 FS/HMMPE [P(TC3 FS 1%)], 1.0 wt% TC3 dark/HMMPE [P(TC3 dark 1%)]

have little influence on the rheological properties of PE in their linear viscoelastic region.

#### Capillary rheometry experiments

As the major experiment in this study, the viscosity reduction abilities of the blends were performed using a pressure-driven rheometer. Here, the controlled piston speed mode was used with round hole capillary dies at 190 °C.

To verify whether the viscosity reduction was due to wall slip, extrusions with the same length to diameter ratio ( $L/D$ ) but different die diameters were investigated. It was

found that the yielding process was a necessary step for any dramatic drop in viscosity. The rheological behaviors of the four blends are plotted with shear stress at wall as a function of apparent shear viscosity in Fig. 9a–d.

According to Mooney's Equation, if die wall slip occurs, the measured apparent shear viscosity is higher for a larger die diameter with the same  $L/D$  ratio at the same apparent shear rate  $\dot{\gamma}_{ap}$ . Figure 9a presents the curves of HMMPE, PT1, and P(TC3 white 1%) blends with two different die diameters and the same  $L/D$  ratio at 190 °C. For the same material, the measured apparent shear viscosity is higher for a smaller die diameter ( $D = 0.7$  mm) with the same  $L/D$  ratio at the same apparent shear rate  $\dot{\gamma}_{ap}$ . This implies that no wall slip took place during the extrusion of this material, prior to the onset of pressure oscillation. Similarly there was no occurrence of wall slip in the P(TC3 dark 1%), P(TC3 FS 1%), and P(TC3 UP 1%) blends with two different dies and the same  $L/D$  ratio tests, as shown in Fig. 9b, c, and d.

In these blends, significant viscosity reductions were initially observed in tests using different die diameters. A yield-like behavior was shown by all blends when the wall stress was almost constant over a region of rapidly decreasing viscosity. In Fig. 10, based on an equivalent wall stress of  $10^5$  Pa, the viscosity reductions at 190 °C with  $L = 21$  and nominal die  $D = 0.7$  mm for the different blends were as follows. The viscosity of PT1 was similar to that of HMMPE, because no yielding (i.e., apparent shear viscosity decreasing with the constant shear stress at wall) occurred; the viscosity of the P(TC3 white 1%) blend was 98.5% (corresponding apparent shear rate 317.6 1/s) of that of HMMPE; for the P(TC3 dark 1%) blend it was 93.0% (corresponding apparent shear rate 87.0 1/s) of that of HMMPE; for the P(TC3 UP) blend it was 92.5% (corresponding apparent shear rate 65.8 1/s) of that of HMMPE; and for the P(TC3 FS 1%) blend it was 97.6% (corresponding apparent shear rate 188.1 1/s) of that of HMMPE.

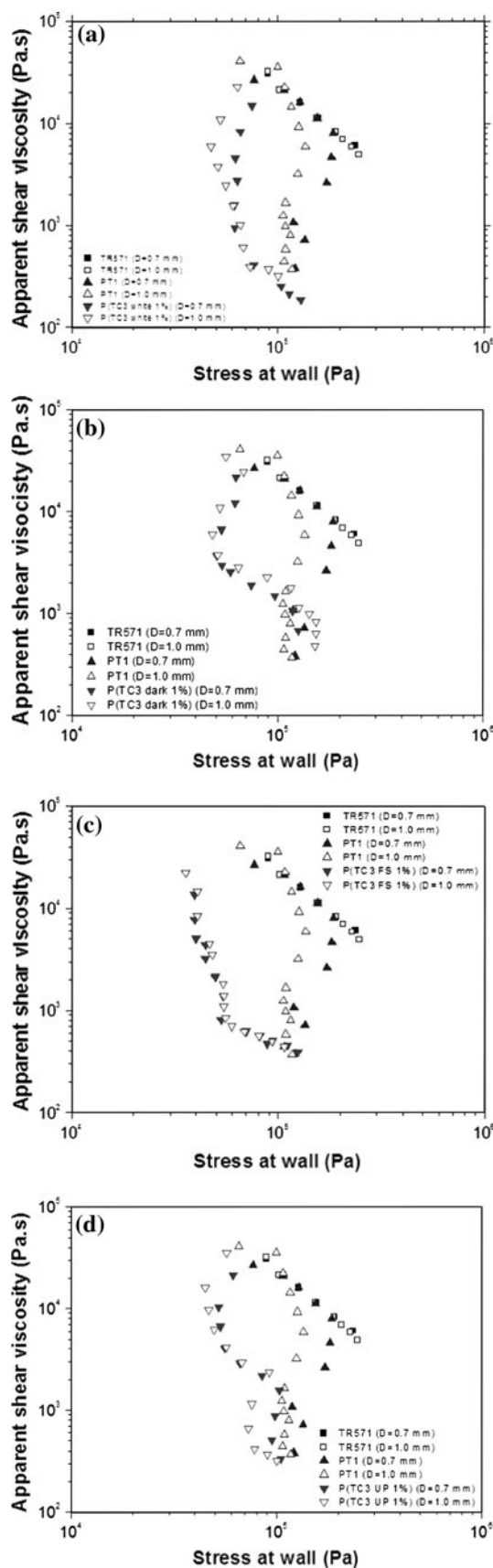
However, yielding stresses and corresponding beginning and ending apparent shear rates were different for each blend. Table 1 gives detailed information about the yielding behaviors of the blends with different capillary rheometry (CR) die diameters. From the table, it is clear that the blends had much lower yielding stress values than PT1. For example, with the same CR die nominal diameter of 0.7 mm, the yielding stress values for the PT1 and organoclay-modified TLCP/HMMPE blends (percentage compared with PT1) were: PT1 was  $1.63 \times 10^5$  Pa; P(TC3 white 1%) was  $0.72 \times 10^5$  Pa (reduced by 56%); P(TC3 dark 1%) was also approximately  $0.72 \times 10^5$  Pa (reduced by 56%); P(TC3 FS 1%) was  $0.53 \times 10^5$  Pa (reduced by 67%); and P(TC3 UP 1%) was  $0.62 \times 10^5$  Pa (reduced by 62%). Also the corresponding apparent shear rates at the beginning of transition were much lower than that of PT1,

**Fig. 9** Apparent shear viscosities as function of shear stress at wall for HMMPE, 1.0 wt% TLCP/HMMPE [PT1] with **a** 1.0 wt% TC3 white/HMMPE [P(TC3 white 1%)], **b** 1.0 wt% TC3 dark/HMMPE [P(TC3 dark 1%)], **c** 1.0 wt% TC3 FS/HMMPE [P(TC3 FS 1%)], **d** 1.0 wt% TC3 UP/HMMPE [P(TC3 UP 1%)] with the same *L/D* ratio (30) and different diameters (0.7 mm and 1.0 mm) at 190 °C with capillary rheometer

which is the reason why it was difficult to obtain the first power-law region in the capillary rheometric tests for the organoclay-modified TLCP/HMMPE blends. For example, with the same CR die nominal diameter of 0.7 mm, the yielding start shear rates were 41.0, 5.6, 2.5, 1.6, and 2.9 1/s for PT1, P(TC3 white 1%), P(TC3 dark 1%), P(TC3 FS 1%), and P(TC3 UP 1%), respectively. The transition regions for the blends were much narrower than those of the PT1, especially for P(TC3 dark 1%) and P(TC3 UP 1%) in the first transition region.

It may be observed that PT1 displayed a higher apparent shear viscosity than HMMPE at a low apparent shear rate. Blends of TLCPs and thermoplastics having higher viscosity than the corresponding pure homopolymer matrix at low shear rates have been reported previously [13–15]. Weiss et al. [13, 14] attributed this to energy dissipation due to the tumbling and rotation of the TLCP domain. In this study, it is clearly demonstrated that a small amount of organoclay in TLCP effectively suppressed the tumbling and rotation of the TLCP domains, and the organoclay-modified TLCP/HMMPE blends displayed lower viscosity than that of HMMPE at low shear rates.

The yielding-like behaviors in all blends presented a slight negative gradient. We suggest that the negative gradient is due to the TLCP phase transition from isotropic to nematic. Theoretically, TLCPs are known to undergo shear-induced phase transitions when the domain orientation is sufficient high [16, 17]. Chan et al. [6] presented the results of optical microscopy/shearing experiments demonstrating a phase transition from isotropic to nematic for this type of TLCP. A pre-translational order in the isotropic phase of a homologous series of liquid crystals close to the isotropic to nematic transition has also been observed experimentally. De Schrijver et al. [18] used a transmission ellipsometric technique to observe this surface-induced isotropic ordering. Here, the negative gradient in PT1 may due to pure isotropic to nematic transition. From previous studies, when a small amount of organoclay is added into TLCP matrix, more or less intercalated structures are formed, especially in TC3 dark hybrid. Under elongated and shear deformation at the entrance and inside CR dies, more nematic phase may be formed due to the ability of the intercalated morphologies of organoclay to maintain order in structures, and this may also be the reason why these blends have a much lower yield stress (or apparent shear



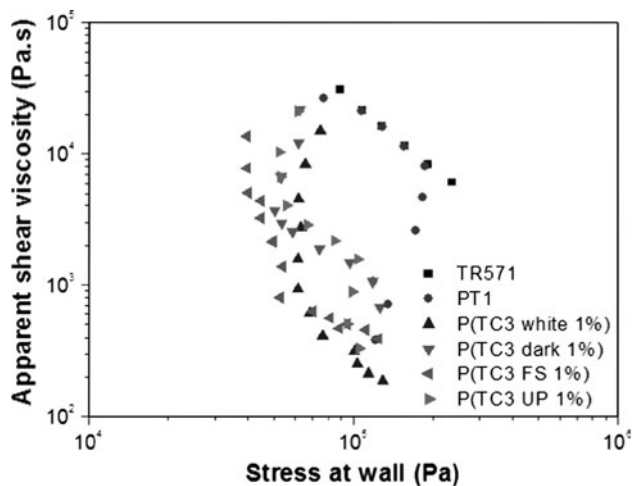


**Fig. 10** Apparent shear viscosities as function of shear stress at wall for HMMPE blends: 1.0 wt% TLCP/HMMPE [PT1], 1.0 wt% TC3 white/HMMPE [P(TC3 white 1%)], 1.0 wt% TC3 UP/HMMPE [P(TC3 UP 1%)], 1.0 wt% TC3 FS/HMMPE [P(TC3 FS 1%)], 1.0 wt% TC3 dark/HMMPE [P(TC3 dark 1%)] with the same  $L/D$  ratio (30) and diameter (0.7 mm) at 190 °C with capillary rheometer

rate). For P(TC3 white 1%) blend, since fully exfoliated organoclay structures were formed in the TLCP, no confinement existed to retain the ordered structure and cause phase transition, long range non-bond forces existed, which also retained more order in the structures, as elaborated in previous study [12].

#### Morphological studies

The SEM diagrams of the etched extrudates are shown in Fig. 11, with magnification of 20,000. For PE, as shown in Fig. 11a, the etched stands create a rough and highly topological contrast. Moreover, a fine line texture is evident after NaOH etching. This indicates that some surface materials or even layers were removed during the etching process. PE is a material that strongly resists NaOH attack. Therefore, the detached material would not be pure PE; otherwise, it would be too easy for the NaOH to diffuse into the PE lattice and remove it from the surface. As has already been illustrated by Chan et al. [7], it is an anti-oxidant-enriched PE layer caused by the migration of

anti-oxidant during shear. Other blends illustrate fine fiber and ellipse patterns. The length of the fibers and the length and width of the ellipses are different in each blend. In these well-defined morphologies, the PT1 strand (Fig. 11b) shows only fibrillar structures, aligned along the flow direction. In the P(TC3 white 1%) strand (Fig. 11c) there are only longitudinal fibrillar striations. In the P(TC3 FS 1%) strand (Fig. 11e) most structures are fibrillar and a few are elliptic (the ratio of ellipse/fiber is low), which was the direct reason why the P(TC3 white 1%) and P(TC3 FS 1%) had similar rheological behaviors, especially in the high frequency region. In the P(TC3 dark 1%) and P(TC3 UP 1%) strands (Fig. 11d, f), many ellipse structures are seen in the images (the ratio of ellipse/fiber is high) and the fibers are wider than in the other blends. The existence of ellipse structures was due partially to agglomeration and relaxation of the TLCP, but was mainly attributable to confinement of the organoclay to TLCP molecules, making it difficult for the TLCP to form fibrillar structures but easier to form elliptic structures in PE during processing in the capillary.

#### Model predictions

From morphological studies, it is clear that irreversible organoclay-modified TLCP droplets deformation in the extensional flow at the capillary entrance and forming fibrillar structures is the reason for the viscosity reduction in organoclay-modified TLCP/HMMPE blends. Previous studies showed that, liquid crystallinity of TLCP in TC3 white and TC3 FS was not affected by the organoclays [19, 20]. P(TC3 white 1%) and P(TC3 FS 1%) should have the similar viscosity reduction mechanism as the TLCP in PE blends. A binary flow pattern model [8], developed based on the experimental observation of strong chain anisotropy in PE melt, due to the presence of highly aligned TLCP molecules within the elongated TLCP domains induced by flow in the TLCP/PE blend system [9], are used to describe the rheological responses of P(TC3 white 1%) and P(TC3 FS 1%) blends. Further development on model prediction of the rheological responses of P(TC3 dark 1%) and P(TC3 UP 1%) will be evaluated later.

**Table 1** Yielding parameters for the blends at 190 °C

	Yielding stress ( $\times 10^4$ Pa)		Yielding start $\dot{\gamma}_{ap}$ (1/s)		Yielding end $\dot{\gamma}_{ap}$ (1/s)	
	0.7	1.0	0.7	1.0	0.7	1.0
Die diameter (mm)	0.7	1.0	0.7	1.0	0.7	1.0
PT1	16.1	13.6	39.8	22.9	–	–
P(TC3 white 1%)	7.08	5.90	6.0	3.5	207.4	110.8
P(TC3 dark 1%)	7.18	5.89	2.51	1.59	18.09	13.58
P(TC3 FS 1%)	5.33	4.11	1.59	0.93	69.74	44.00
P(TC3 UP 1%)	6.15	5.72	2.89	1.61	23.15	13.58

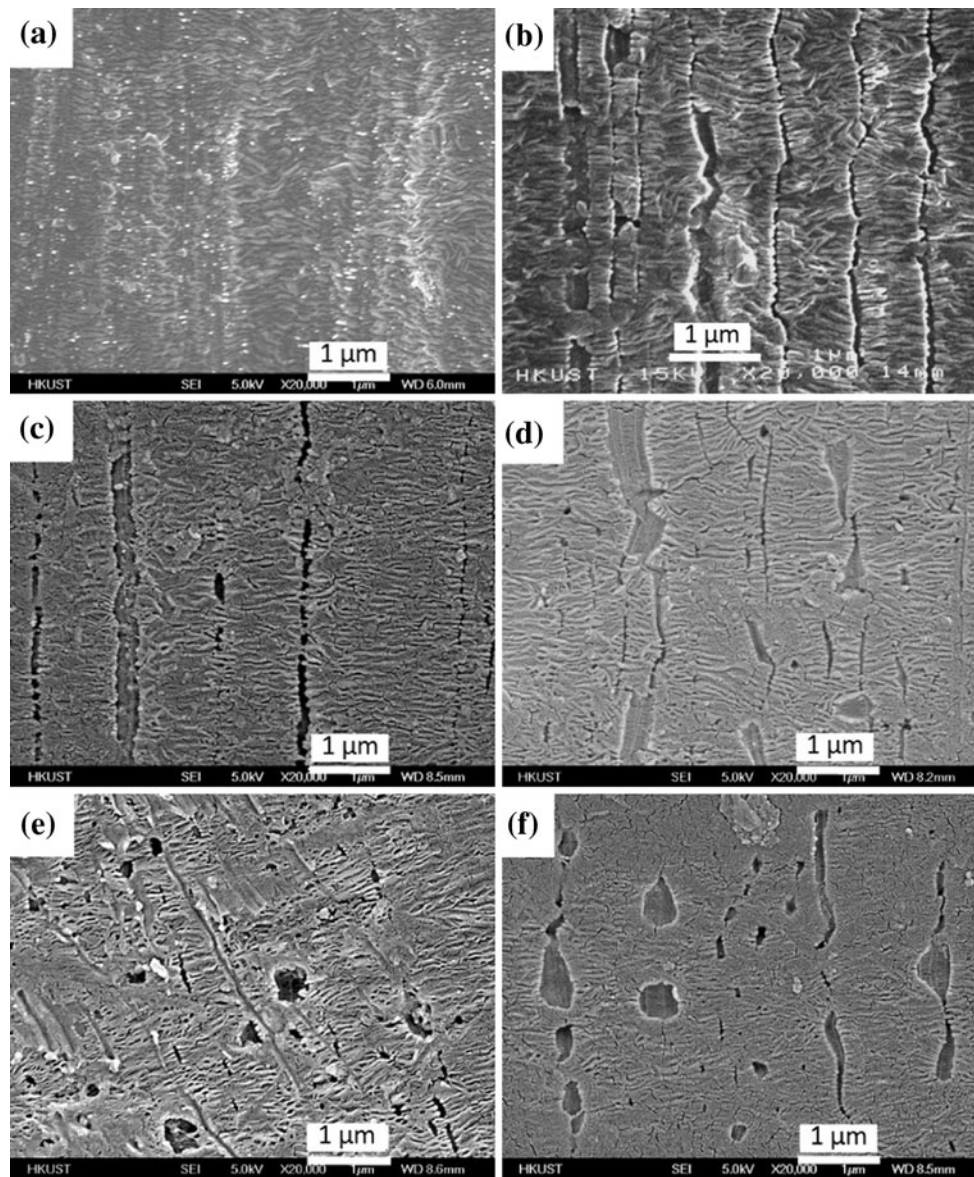


**Fig. 11** SEM images of **a** HMMPE, **b** 1.0 wt% TLCP/HMMPE [PT1], **c** 1.0 wt% TC3 white/HMMPE [P(TC3 white 1%)], **d** 1.0 wt% TC3 dark/HMMPE [P(TC3 dark 1%)], **e** 1.0 wt% TC3 FS/HMMPE

[P(TC3 FS 1%)], and **f** 1.0 wt% TC3 UP/HMMPE [P(TC3 UP 1%)] with magnification 20,000 $\times$

Figure 12a, b, and c shows the schematic diagrams of velocity profile development of the blends in the capillary die [8]. In the regions I, a homogeneous highly viscous melt (with random coil chains) exists where the maximum fluid velocity (in the center of the die) is below the critical velocity. Its velocity profile (named with pattern B) is shown in Fig. 12a. The regions III, a homogeneous low viscous melt (with the extended chains conformation) exists, where the minimum fluid velocity (at the wall of the die) is above the critical velocity. The velocity profile (named with pattern A) is shown in Fig. 12c. Its velocity profiles of patterns B and A in region I and III can be obtained by using the simple power-law constitutive relation and the non-slip boundary conditions at wall.

In the region II (or the intermediate transition region) with constant shear stress at wall plateau, the melt in the center region flows at velocities above the critical velocity for chain disengagement, Fig. 12b. As the centerline velocity exceeds a critical value, the corresponding elongation rate is high enough to stretch the PE chains along the center core, from the random coil conformation to the extended chain conformation [9]. Pattern A starts to develop in the center core and the melt transforms into the binary flow pattern, as Fig. 12b shows. As apparent shear rate increases, the pattern A expands toward the capillary die wall until it touches the wall. At this point, region III achieves. The velocity profile for the region II is obtained

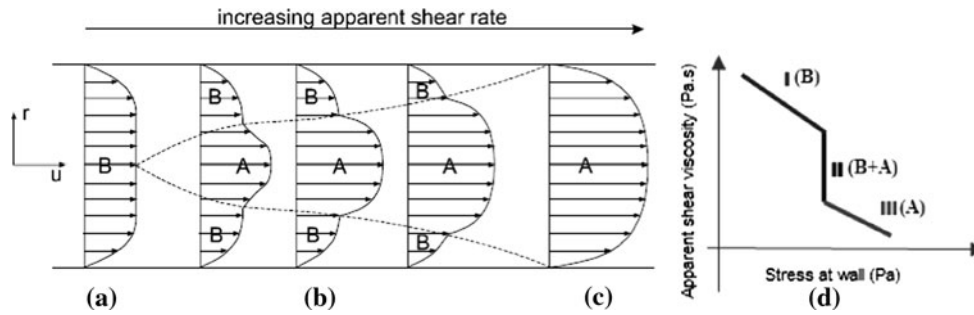


**Fig. 12** Schematic diagram illustrating the flow regimes characterized by alternating flow patterns A and B as a function of maximum fluid velocity developed from the center region [8]. **a** Region I, a homogeneous highly viscous melt where the maximum fluid velocity (occurred in the center) is below the critical velocity; **b** Region II, the melt in the center region flows at a velocity above the critical velocity

for chain disengagement; **c** Region III, a homogeneous low viscous melt where the minimum fluid velocity (occurred at wall) is above the critical velocity; and **d** schematic apparent shear viscosity evolution as a function of stress at wall at different regions (I, II, and III) in capillary die at 190 °C

by assuming interfacial continuity in velocity and shear stress. As the shear rate increases, the center core region characterized by the low viscosity melt flow characteristics expands from the center core toward the die wall. Close to the wall, the velocity profiles are independent of apparent shear rates. This implies that the shear rate at the wall is independent of the flow rate of fluid during the melt structure transition period. Consequently, the wall shear stresses will remain constant throughout this transition period (region II). Figure 12d shows the schematic drawing of the corresponding apparent shear viscosity as a function of shear stress at wall at the different regions described by the model in the capillary die.

The power-law constitutive relation inside the capillary die can be defined:

$$\tau = \frac{\Delta P r}{L 2} = K \left( -\frac{du}{dr} \right)^n \tag{1}$$

where, the shear stress at wall  $\tau$  (at an arbitrary radius  $r$ ) inside a round-hole capillary of radius  $R$  and length  $L$  is proportional to the overall pressure drop gradient  $\Delta P/L$  (measured by experiments).  $K$  and  $n$  are the power-law constants fitted by the experimental data.

The velocity profiles of patterns A and B in region I and III:

$$u = CC_R \left[ 1 - \left( \frac{r}{R} \right)^{(n+1)/n} \right] \tag{2}$$

where,  $C = (\Delta P/2KL)^{1/n} (n/(n+1)) = ((3n+1)/4(n+1)) (\dot{\gamma}_{ap}/R^{1/n})$  and  $C_R = R^{(n+1)/n}$ .

The velocity in region II with interfacial continuity in velocity and shear stress:

$$u = u_I + C_A C_{R,A} \left[ \left( \frac{r_1}{R} \right)^{(n_A+1)/n_A} - \left( \frac{r}{R} \right)^{(n_A+1)/n_A} \right] \text{ for } r < r_1$$

$$u = C_B C_{R,B} \left[ 1 - \left( \frac{r}{R} \right)^{(n_B+1)/n_B} \right] \text{ for } r_1 \leq r \leq R \tag{3}$$

where  $u_I = C_B C_{R,B} \left[ 1 - \left( \frac{r_1}{R} \right)^{(n_B+1)/n_B} \right]$  and subscripts A and B stand for parameters in region III and region I.

Critical shear stress in region II:

$$u_{0,cr} = C_B C_{R,B} = \frac{3n_B + 1}{4(n_B + 1)} R \dot{\gamma}_{ap,cr}$$

$$\tau_{w,cr} = K_B \dot{\gamma}_{ap,cr}^{n_B} = K_B \left( \frac{4(n_B + 1)u_{0,cr}}{3n_B + 1 R} \right)^{n_B} \tag{4}$$

where  $\dot{\gamma}_{ap,cr}$  refers to the critical apparent shear rate at the onset of transition to region II flow;  $u_{0,cr}$  refers to the minimum velocity for transition; and  $\tau_{w,cr}$  refers to the critical shear stress at wall in region II.

The typical velocity profile developments of fluid flowing through capillary dies for nominal  $D = 1.0$  mm are shown in Fig. 13. In the velocity profiles for different blends, the real die diameters were used rather than the nominal diameter. For the nominal diameters 1.0 and 0.7 mm, the real calibrated diameters were 0.924 and 0.542 mm.

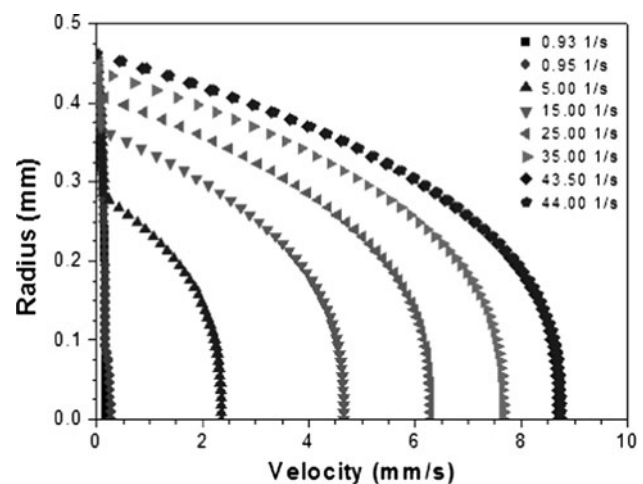


**Fig. 13** Velocity profile development in region II of flow at  $R = 0.462$  mm for 1.0 wt% TC3 FS/HMMPE [P(TC3 FS 1%)] at 190 °C by simulation

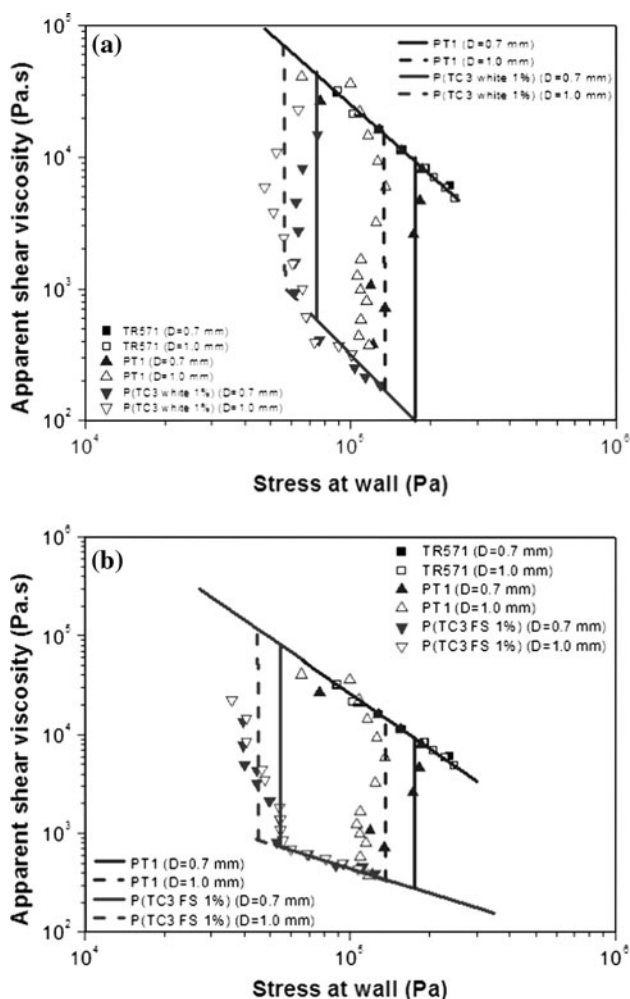


**Fig. 14** Apparent shear viscosities as function of shear stress at wall for HMMPE, 1.0 wt% TLCP/HMMPE [PT1], **a** 1.0 wt% TC3 white/HMMPE [P(TC3 white 1%)] and **b** 1.0 wt% TC3 FS/HMMPE [P(TC3 FS 1%)] with the same *L/D* ratio (30) and different diameters (0.7 mm and 1.0 m) at 190 °C with capillary rheometer. (The points were measured data and the curves were simulated data.)

Precise flow curves with Matlab program simulation for the blends are plotted in Fig. 14a and b together with experimental data, excellent agreement between model prediction and experimentally measured flow curves was obtained.

**Conclusion**

Small amounts of organoclays of different sizes and concentrations were added into thermotropic liquid crystalline

polymer (TLCP) to form four typical types of organoclay-modified TLCPs: TC3 white, TC3 dark, TC3 FS, and TC3 UP. Acting as viscosity reduction agents, 1.0 wt% of each of these organoclay-modified TLCPs, was blended into high molecular mass PE (HMMPE) matrix. These blends had dramatically different rheological properties from those of HMMPE and the 1.0 wt% TLCP/HMMPE blend [PT1], and they were also different from each other. The organoclay-modified TLCPs blends displayed lower viscosity, yield stress and yielding apparent shear rate and narrower yielding apparent shear rate region than those of PT1. The organoclays also functioned as stabilizers, suppressing the tumbling and rotation of the TLCP in HMMPE during processing at low shear rates. Fibrillation was still the main reason for viscosity reduction. The binary flow pattern model was applied for prediction of the rheological properties of PT1, TC3 white/HMMPE, and TC3 FS/HMMPE blends, with excellent consistency.

**Acknowledgement** This project was funded by a grant from the Research Grant Council of Hong Kong, Grant number HKUST6256/02.

**References**

1. Kim WM, Denn MM (1992) *J Rheol* 36:1477
2. Brostow W, Sterzynski T, Triouleyre S (1996) *Polymer* 37:1561
3. Kohli A, Chung N, Weiss RA (1989) *Polym Eng Sci* 29:573
4. Handlos AA, Baird DG (1995) *J Macromol Sci Rev Macromol Chem* C35:183
5. Whitehouse C, Lu XH, Gao P, Chai CK (1997) *Polym Eng Sci* 37:1944
6. Chan CK, Whitehouse C, Gao P (1999) *Polym Eng Sci* 39:1353
7. Chan CK, Whitehouse C, Gao P, Chai CK (2001) *Polymer* 42:7847
8. Chan CK, Gao P (2005) *Polymer* 46:8151
9. Chan CK, Gao P (2005) *Polymer* 46:10890
10. Tang YH, Yang HM, Gao P (2007) *J Cent South Univ Technol* 14:192
11. Tang YH, Gao P, Ye L, Zhao CB (2010) *Polym Eng Sci* (accepted)
12. Tang YH, Gao P, Ye L, Zhao CB, Lin W (2010) *J Mater Sci* 45:2874. doi:10.1007/s10853-010-4277-y
13. Weiss RA, Wansoon H, Nicolais L (1987) *Polym Eng Sci* 27:684
14. Weiss RA, Wansoon H, Nicolais L (1988) *High modulus polymers*. Marcel Dekker, New York, pp 145–147
15. Nobile MR, Amendola E, Nicolais L, Acierno D, Carfagna C (1989) *Polym Eng Sci* 29:244
16. Mather PT, Romo-Uribe A, Han CD, Kim SS (1997) *Macromolecules* 30:7977
17. Han CD, Kim SS (1995) *Macromolecules* 28:2089
18. de Schrijver P, van Dael W (1996) *J Thoen Liq Cryst* 21:745
19. Tang YH, Gao P, Ye L, Zhao CB (2010) *Polymer* 51:514
20. Tang YH, Gao P, Ye L, Zhao CB (2010) *J Polym Sci B* 48:712